

Systematic Study of Shell Effect near Drip-lines

S. Adhikari^a and C. Samanta^{a,b}

^a*Saha Institute of Nuclear Physics,
1/AF Bidhannagar, Kolkata 700 064*

and

^b*Physics Department, Virginia Commonwealth University
Richmond, Virginia 23284-2000*

Variation of nuclear shell effects with nucleon numbers are evaluated using the modified Bethe-Weizsäcker mass formula (BWM) and the measured atomic masses. The shell effects at magic neutron numbers $N=8, 20, 28, 50, 82$ and magic proton numbers $Z=8, 20, 28, 50$ and 82 are found to vary rapidly approaching the drip lines. The shell effect increases when approaches another magic number. Thus, shell effects are not always negligible near the drip lines.

Keywords: Binding energy, mass formula, shell effect.

With increasing discoveries of more and more nuclei away from the valley of stability, the domain of nuclear-magicity has started changing. In neutron (N) or, proton (Z)-rich nuclei unusual stabilities are found at various N or, Z values which are very different from the well known magic numbers $2, 8, 20, 28, 50, 82$ and 126 [1, 2]. On

the other hand, loss of magicity at $N=8$ ($Z=4$) [2] has been experimentally confirmed [3]. Quenching or, loss of magicity in nuclei away from the valley of stability is a topic of great current interest because of its direct relevance to the production of heavy elements both in the laboratory and at the astrophysical sites. Chen et al. showed [4] that theoretical calculations incorporating quenching of the $N=82$ shell gap for $Z < 50$ nuclei leads to a filling of the known abundance troughs around $A \sim 120$ and 140 and generates a better overall reproduction of the heavy elements. However, there are still some discrepancies which calls for further investigation. As quenching of magic shell gap near n- and p-drip line would have significant effect on the astrophysical processes, a systematic study of the possible quenching of the magic shell effects away from the valley of stability is essential. In this work we present a systematic study of the possible change of shell effects for nucleon number $8, 20, 28, 50, 82$ and $N=126$ through a comparison of experimental data and results from a mass formula without shell effect.

A mass formula based on the liquid drop model was first prescribed by Bethe-Weizsäcker (BW) [5, 6, 7]. It was designed to fit the heavy and medium mass nuclei. As it has no shell correction incorporated the BW fails near the magic numbers where the closed shell structure of nuclei demands extra stability. For years this inadequacy has been utilized to identify the magic numbers as they stand out as marked deviations [5, 6, 7]. With the discovery of nuclei away from the valley of stability it was noticed that the BW formula is inadequate near the drip lines,

especially for light nuclei [2]. The improved liquid drop model (ILDm) [8] also does not reproduce the trend of the binding energy versus neutron number curves of light nuclei correctly. Earlier we suggested a modified Bethe-Weizsäcker mass formula (BWM) in which the binding energy is defined in terms of mass number A ($=N+Z$) and proton number (Z) as [2],

$$BE(A, Z) = 15.777A - 18.34A^{2/3} - 0.71 \frac{Z(Z-1)}{A^{1/3}} - \frac{23.21}{(1 + e^{-A/17})} \times \frac{(A-2Z)^2}{A} + (1 - e^{-A/30})\delta, \quad (1)$$

where, $\delta = +12 A^{-1/2}$ for even Z -even N nuclei, and $-12 A^{-1/2}$ for odd Z -odd N nuclei and 0 for odd A nuclei. The BWM reproduces the general trend of the binding energy versus neutron number curves for all nuclei from Li to Bi. Like BW, the BWM also does not contain any shell correction or Wigner term [9]. Therefore, it overpredicts the mass near the magic numbers as well as for nuclei with $N=Z$. As the shell effect quenches, the discrepancy between the experimental data and the predictions of BWM diminishes. Therefore BWM can be used to identify extrastability as well as, quenching of shell effect through a comparison with the experimental mass data. In the following, we study the change of shell effects with nucleon numbers near the magic numbers 8, 20, 28, 50, 82 and 126 using the BWM and experimental mass data [10, 11, 12].

The one nucleon separation energy of a nucleus (A, Z) is defined as,

$$S_n(A, Z) = BE(A, Z) - BE(A-1, Z) \quad (2)$$

$$S_p(A, Z) = BE(A, Z) - BE(A - 1, Z - 1) \quad (3)$$

When this S_n or, S_p are plotted against N or Z , a large drop is found after the N or Z values which correspond to magic numbers. BWM cannot reproduce this break as it has no shell effect incorporated. Fig.1(a) and Fig. 1(b) show one-neutron separation energy (S_n) versus neutron number plots for Be($Z=4$) and O($Z=8$). For O($Z=8$) (Fig.1b), a large break at $N=8$ is clearly seen in experimental data which is not reproduced by BWM. On the otherhand, for $Z=4$ there is no large break in the experimental data at $N=8$ and, the difference between the BWM and experimental data almost disappears. This indicates loss of $N=8$ magicity in $Z=4$ nucleus and it has been experimentally confirmed [3]. Incidentally a large break can be seen in the experimental data at $N=4$ for Be($Z=4$), which arises due to extrastability of $N=Z$ nuclei. BWM cannot reproduce this large break as Wigner term is not incorporated in BWM. Similar zones of quenching of shell effects can be seen by plotting the one-nucleon separation energy derived from experimental data and the BWM predictions [13]. The difference (ΔB) between the experimental binding energies (BE(EXP)) and theoretical (BE(BWM)) ones are computed using experimental masses [10, 11, 12] and the mass formula BWM. In Fig.1(d) it can be seen that ΔB has a large value at neutron magic number $N=8$ whereas, no such peak can be seen at $N=8$ for Be (Fig. 1(c)). This delineates the expected magicity at $N=8$ for $Z=8$ and, the loss of $N=8$ magicity at $Z=4$. In Fig. 1(c) the extrastability at $N=Z=4$ and at magic number $N=2$ are clearly seen. The new magic number $N=16$ [1, 2] also emerges clearly (Fig. 1(d)) in this comparison with the experimental data and

BWM.

The two nucleon separation energy (S_{2i} , $i=n,p$), the so-called, "shell gap" (G_{2i}) and the "shell effect" (ΔB) of a nucleus (A,Z) are defined as,

$$S_{2n}(A, Z) = BE(A, Z) - BE(A - 2, Z) \quad (4)$$

$$S_{2p}(A, Z) = BE(A, Z) - BE(A - 2, Z - 2) \quad (5)$$

$$\begin{aligned} G_{2n}(A, Z) &= S_{2n}(A, Z) - S_{2n}(A + 2, Z) \\ &= 2BE(A, Z) - BE(A - 2, Z) - BE(A + 2, Z) \end{aligned} \quad (6)$$

$$\begin{aligned} G_{2p}(A, Z) &= S_{2p}(A, Z) - S_{2p}(A + 2, Z + 2) \\ &= 2BE(A, Z) - BE(A - 2, Z - 2) - BE(A + 2, Z + 2) \end{aligned} \quad (7)$$

$$\Delta B = BE(EXP) - BE(BWM) \quad (8)$$

The G_{2i} is usually plotted with the experimental mass data [10, 11, 12] to monitor the change of shell gap, but it can not be used if there is a drastic change of shape in nuclei associated with the evaluation of G_{2i} . Whereas, the ΔB being simply the difference between the experimental and theoretical mass is not affected by the deformation of other nuclei.

Plots of G_{2n} versus proton number for $N=8, 20, 28, 50, 82$ and 126 are shown in Fig.2 . Similar plots of G_{2p} versus neutron number for $Z=8, 20, 28, 50$ are presented in Fig.3. The mass formula BWM, which has no shell correction or, Wigner effect incorporated, predicts a smooth continuous line and thus acts as a base line for

comparison. There are several interesting features in the G_{2i} plots. The so called "shell gap" of all these magic numbers appears to change with nucleon numbers but they peak at N or, Z values where they get support from another magic number. The extrastability is found to decrease on both sides of the main peak. In Fig.2 a rise in experimental G_{2n} values above the BWM predictions is seen for $N=8(Z=7-9)$, $N=20(Z=10, 15-17, 19-21)$, $N=28(Z=15, 16, 18-24, 27-32)$. The shell effects for $N=50, 82$ and 126 do not disappear in the existing experimental data. For $N=28$, three peaks are seen at $Z=16, 20, 28$ of which the last two are known magic numbers. In Fig.3 similar rise is seen for $Z=8(N=7-9, 13-16)$, $Z=20(N=19-21, 27-31, 33)$. For $Z=28$, BWM overpredicts only at $N=25$ and for $Z=50$, the experimental G_{2p} values are always far above BWM. A comparison with the predictions of BWM indicates strong quenching of G_{2n} at $N=8(Z=4-6, 10)$, $N=20(Z=11-14, 18, 22-24)$, $N=28(Z=17, 25, 26, 30)$. Some quenching is seen at $N=50(Z=32)$, $N=82(Z=49)$, $N=126(Z=81, 80, 83-90)$. Similar quenching of G_{2p} can be seen for $Z=8(N=6, 10-12)$, $Z=20(N=16-18, 22-26)$, $Z=28(N=25)$.

The plot of G_{2p} for $Z=82$ is presented in Fig.4 along with predictions of different mass formulae [2, 14, 15, 16, 8]. The experimental G_{2p} value queches on both sides of the peak at $N=126$. At $N = 106$ the difference between experimental value and BWM prediction almost vanishes (~ 140 keV) but, increases again at $N<106$. Interestingly, the recent mass formula of Koura et al. [15], which is known to be valid for both light and heavy nuclei, reproduces most of the details of the experimental data

for G_{2i} distributions of lower magic numbers (Fig.2 and 3). But for heavier nuclei it delineates significant overprediction near drip lines and under prediction near the peaks. Results from the mass formula of Möller et al. [16], Satpathy-Nayak [14] and ILDM [8] are also enclosed for comparison. Although they have shell correction incorporated, none of them reproduces the exact nature of the G_{2p} distribution of $Z=82$.

In Fig.5, the difference (ΔB) between the binding energies computed from the experimental masses [10, 11, 12] and the BWM is plotted against the proton numbers for neutron magic nuclei. Similar plot for the proton magic nuclei are presented in Fig. 6 against the neutron numbers. The BWM being basically a liquid drop model without shell effect acts as the base line for evaluation of the shell effect in nuclei. From these figures it is clear that the shell effect does not always quench near the drip lines. In some nuclei the shell effect, after a quenching near the mid shell region, actually increases near the drip line as another magic number is approached. In Fig. 5, for $N=8$, the extrastability disappears for $Z=3-5$. It is interesting to note that in Fig. 5, $N=28$ shows extrastability at $Z=28, 20$ and a mild increase towards $Z=16$ and, the fall after $Z=28$ is rather flat in the region $Z=31-33$. In Fig. 6, for $Z=16$, the extrastability does not reduce after the magic neutron number $N=28$. On the contrary, at $N=32$ it is even higher. For $Z=20$ in Fig. 6, the $N=29, 31$ and 33 have higher ΔB values than $N=28$. This suggests that the neutron magic number in this region might be at higher N values. New magicities at $N=30$ and 32 have been

predicted earlier around $Z=20$ region [17]. However, as some of these data points are from systematics only, additional mass measurement for neutron-rich Sulfur isotopes are needed to confirm this probable shift of neutron magicity.

From Figs. 3, 4 and Figs. 5, 6 it is clear that quenching or, loss of shell effects or, extrastability demonstrated by ΔB and G_{2p} are not always the same. The reason for this anomaly is the way they are evaluated. The evaluation of G_{2p} at each point involves masses of three nuclei. Therefore, its use as a measure of shell gap is restricted if there is a drastic change in shape or, deformation in any of the three nuclei. The ΔB gives the measure of the shell effect (not the shell gap), and it involves only the mass of one nucleus at each point.

Recently, experimental evidence of $N=82$ shell quenching has been claimed by observing the high Q_β value for ^{130}Cd [18] which can not be explained by the "unquenched" finite-range droplet model(FRDM). In one-neutron separation energy versus N plot (Fig.7) one can see the large break at $N=82$ for the magic nucleus Sn ($Z= 50$) which can not be reproduced by BWM, as expected. Similar break in Te ($Z=52$) is seen at $N=82$, but with a lesser magnitude. Like the Sn and Te, the S_n versus N data for Cd also shows a gradually increasing discrepancy between the experimental data and BWM as it approaches the magic number $N=82$ beyond which no experimental mass data is available so far. It only shows a large break at $N=50$ indicating existence of large shell effect at $N=50$ for $Z=48$. Measurements

of the mass of $^{129,131,132}\text{Cd}$ are essential to see whether there is a break in S_n after $N=82$ and how big it is. In view of the predicted quenching of $N=82$ shell gap in Cd, a considerable reduction in this break is expected.

In summary the change of shell effects in nuclei with N or $Z=8, 20, 28, 50, 82$ and $N=126$ approaching the drip lines have been studied. A modified Bethe-Weizsäcker mass formula (BWM)[2] is employed for comparison. The BWM reproduces the general trend of the binding energy versus nucleon number curves for Li to Bi nuclei much better than the existing macroscopic formulas. It has no shell effect incorporated. If the shell effect quenches, the discrepancy between the BWM predictions and experimental data diminishes. Thus BWM serves as a baseline for comparison. The G_{2i} and ΔB values are used here to monitor the change of shell effects with change of neutron and proton numbers. Mass formulae of Koura et al. [15], Möller et al. [16] and Satpathy-Nayak [14], which have built in shell effects, are used for comparison. The shell effects are found to vary with the nucleon numbers and increase if it approaches another magic number. Several domains of shell effect quenching and extrastability are found for $Z=4, 6, 8, 16, 20, 28, 82$ and $N=6, 8, 16, 20, 28, 82$ and 126 of which loss of magicity at $N=8(Z=4)$ shown here is already confirmed experimentally. Further experimental data are needed to confirm many of the observations suggested by this work.

Bibliography

- [1] A.Ozawa et al., Phys. Rev. Lett. **84**, 5493 (2000)
- [2] C.Samanta and S.Adhikari, Phys.Rev.C **65**, 037301 (2002); see references therein
- [3] A.Navin et al., Phys. Rev. Lett. **85**, 266 (2000)
- [4] B.Chen et al., Phys. Lett. **B 355**, 37 (1995)
- [5] Kenneth S.Krane, "*Introductory Nuclear Physics*", John Wiley & Sons, 1987
- [6] K.Heyde, "*Basic ideas and concepts in nuclear physics*", IOP publication, 1999
- [7] M.A.Preston and R.K.Bhaduri, "*Structure of the Nucleus*", Addison-Wesley Publishing Company, 1975
- [8] S. R. Souza et al., Phys.Rev.C **67**, 051602(R) (2003);
- [9] E.P.Wigner, Phys. Rev. **51**, 106 (1937)
- [10] Nuclear Wallet Cards, Brookhaven National Laboratory, 2000
- [11] Yu. N. Novikov et al., Nucl. Phys. **A697**, 92 (2002)

- [12] S.Schwarz et al., Nucl. Phys. **A693**, (2001) 533
- [13] D. N. Basu, Private communication;IJMPE (in press)
- [14] L.Satpathy and R.Nayak, Phys. Rev. Lett. **51**, 1243 (1983)
- [15] H.Koura, M.Uno, T.Tachibana and M.Yamada, Nucl. Phys. **A 674**, 47 (2000)
- [16] P.Möller, J.R.Nix, W.D. Myers and W.J. Swiatecki, Atomic Data and Nuclear Data Tables **59**, 185 (1995)
- [17] Rituparna Kanungo, I.Tanihata and A.Ozawa, Phys. Lett. B **528**, 58 (2002)
- [18] I.Dillmann et al., Phys. Rev. Lett. **91**, 162503 (2003)

Figure Caption :

Fig. 1(a),(b) Plots of one-neutron separation energy(S_n) versus neutron number(N) curve from experimental data [10] and BWM to delineate strength of shell effect at $N=8$ for $Z=4, 8$; **(c),(d)** plots of ΔB ($=BE(EXP)-BE(BWM)$) versus neutron number(N) curve from experimental data [10] and BWM to delineate strength of shell effect at $N=8$ for $Z=4, 8$.

Fig. 2 Plots of $G_{2n} = S_{2n}(N) - S_{2n}(N+2)$ versus proton number (Z), computed from measured masses [10, 11] and from the mass formulas of BWM [2], Koura et al. [15], and Möller et al. [16] for magic neutron numbers $N=8, 20, 28, 50, 82$ and 126.

Fig. 3 Plots of $G_{2p} = S_{2p}(Z) - S_{2p}(Z+2)$ versus neutron number, computed from measured masses [10, 11] and from the mass formulas of BWM [2], Koura et al. [15], and Möller et al. [16] for magic proton numbers $Z=8, 20, 28, 50$.

Fig. 4 Plots of G_{2p} from measured mass [10, 11, 12] and from the mass formula of BWM [2], Satpathy-Nayak [14], Koura et al. [15], and Möller et al. [16] for magic proton number $Z=82$.

Fig. 5 Plots of ΔB versus proton number(N) from experimental data [10, 11, 12] and BWM to show the variation of shell effects for $N=6, 8, 16, 20, 28, 50, 82$ and 126.

Fig. 6 Plots of ΔB versus neutron number(N) from experimental data [10, 11, 12] and BWM to show the variation of shell effects for $Z=6, 16, 20, 28, 50, 82$.

Fig. 7 Plots of one-neutron separation energy(S_n) versus neutron number(N) curve

from experimental data [10] and BWM for Cd($Z = 48$), S_n ($Z = 50$) and, Te($Z = 52$).

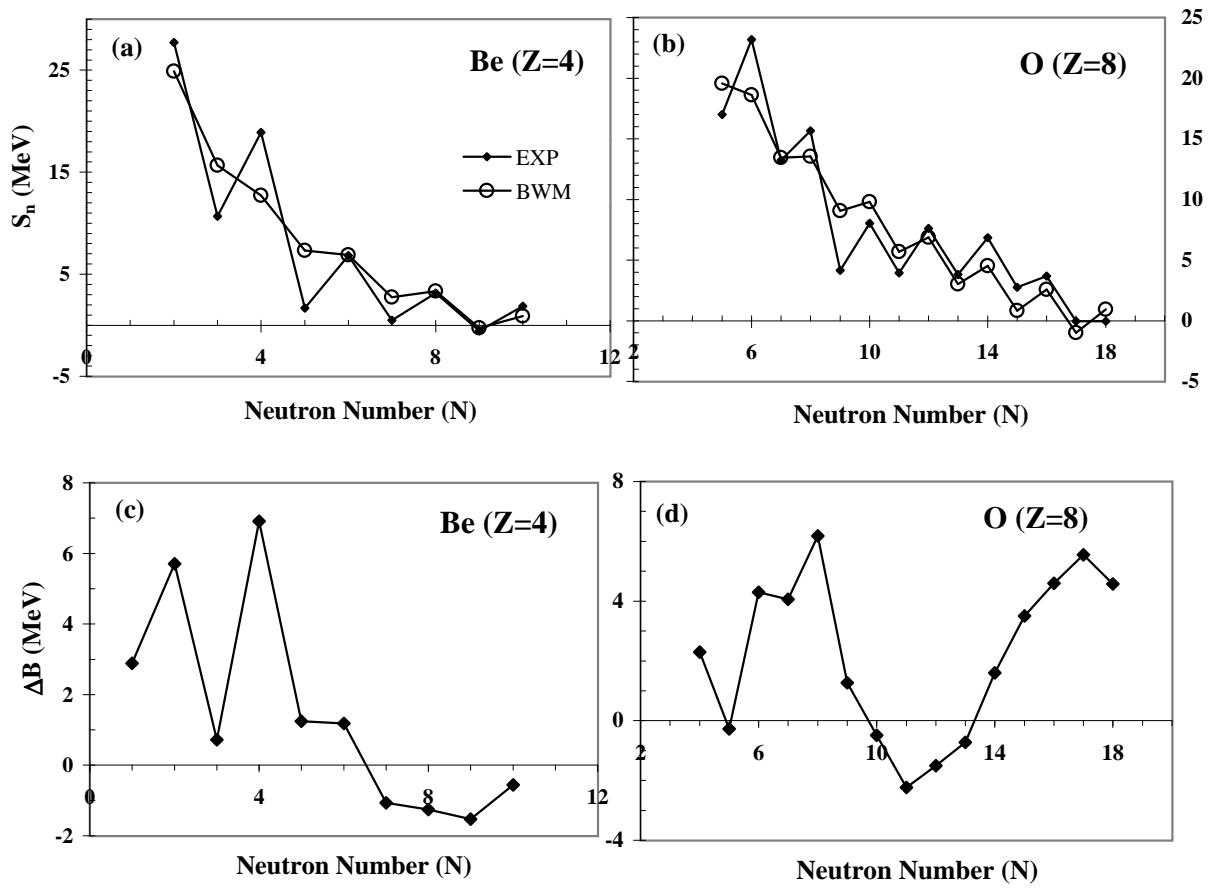


Fig. 1

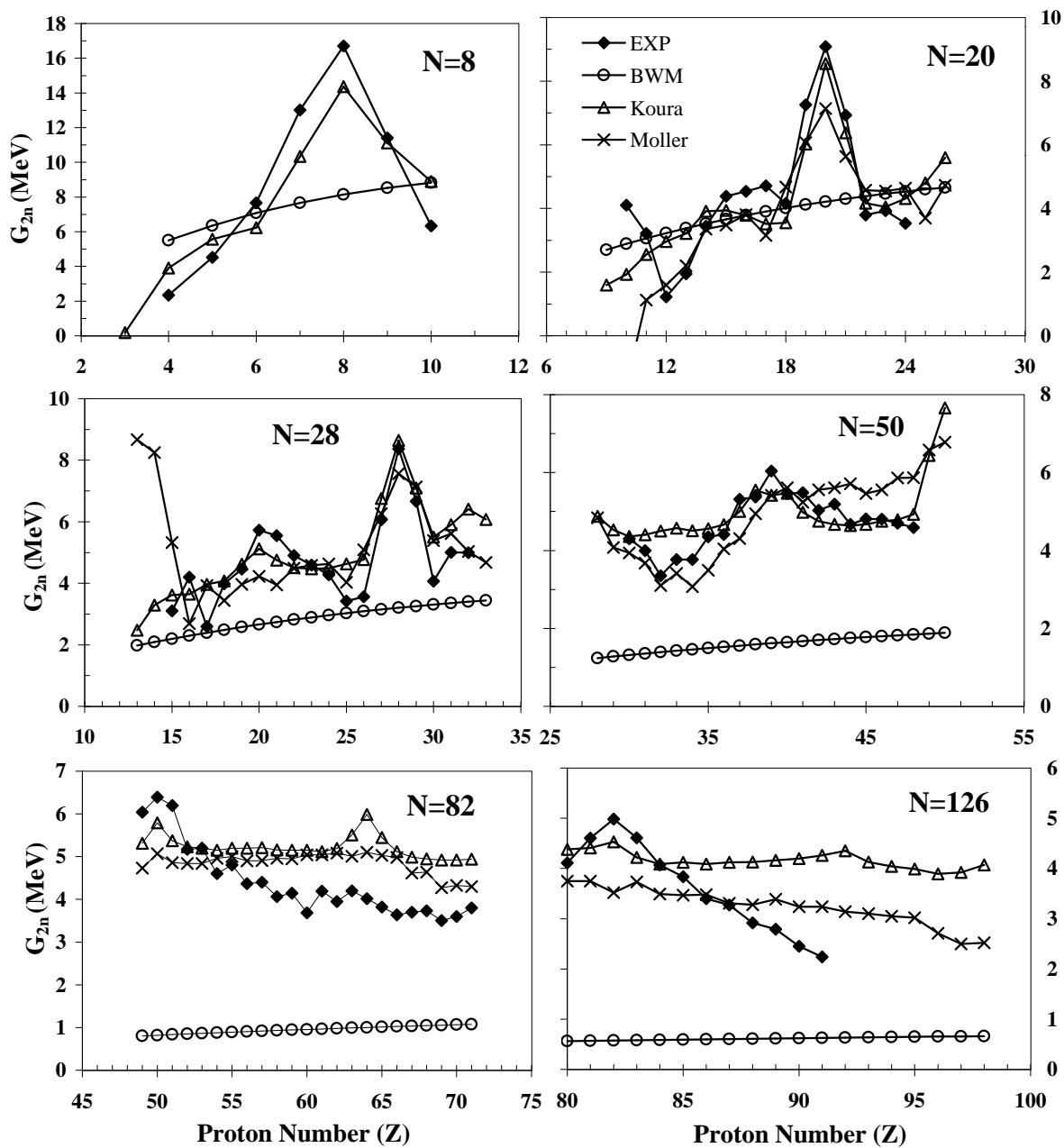


Fig. 2

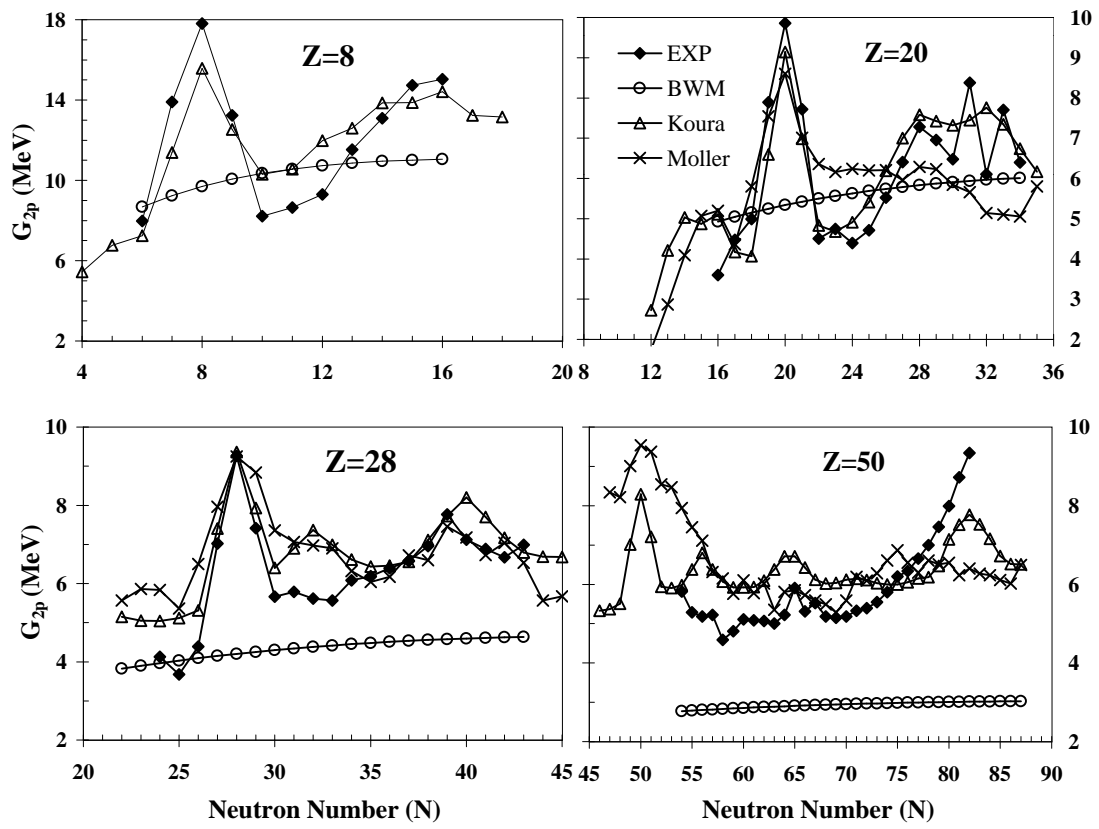


Fig. 3

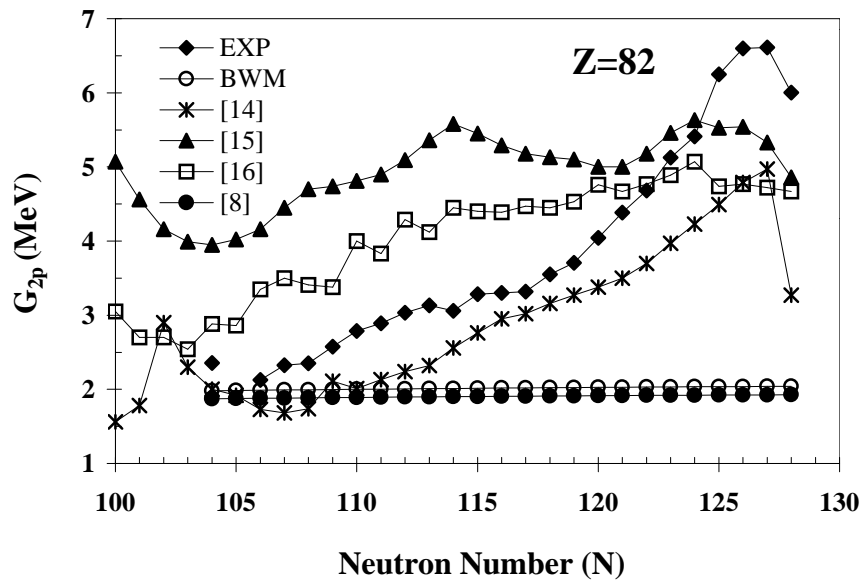


Fig. 4

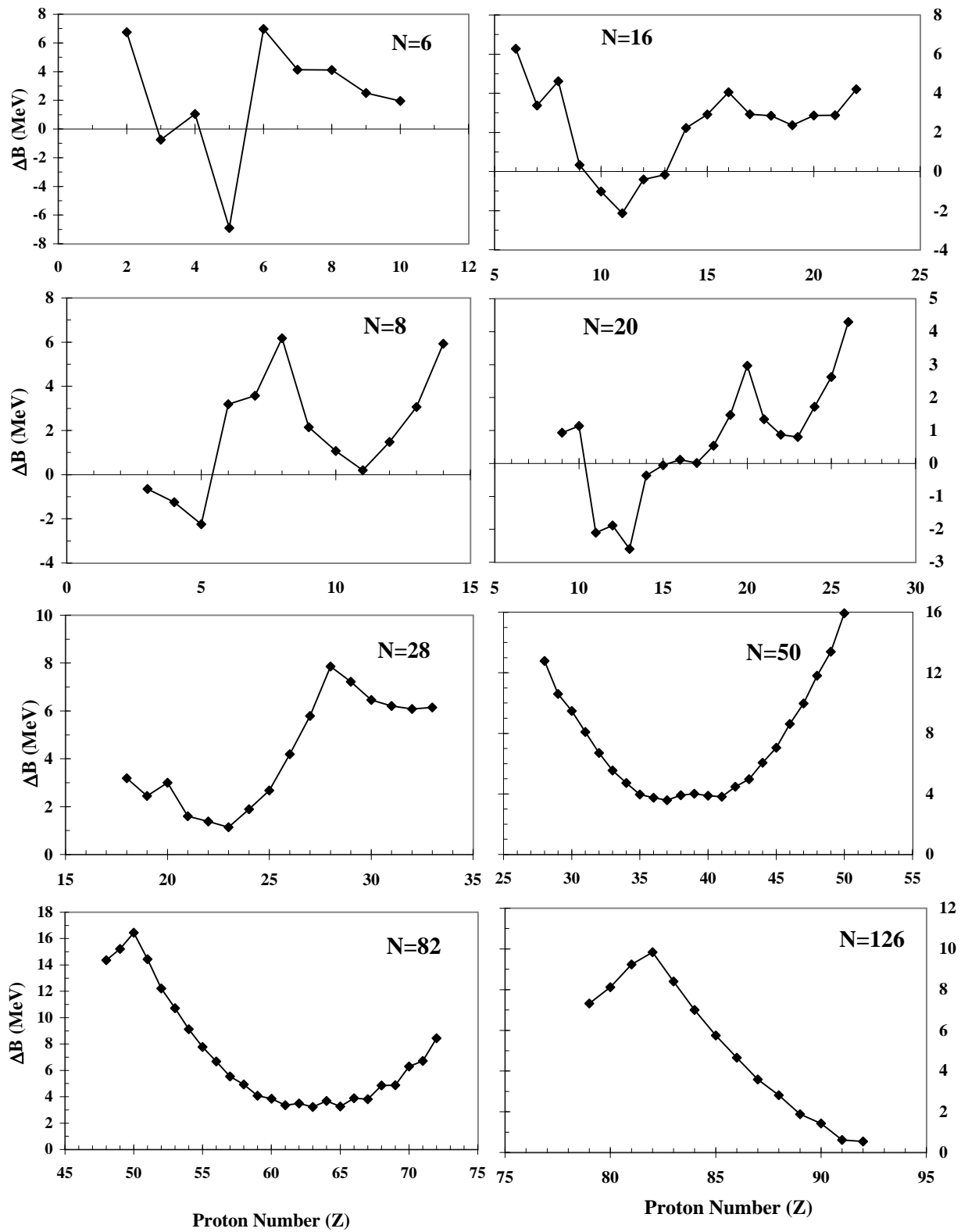


Fig.5

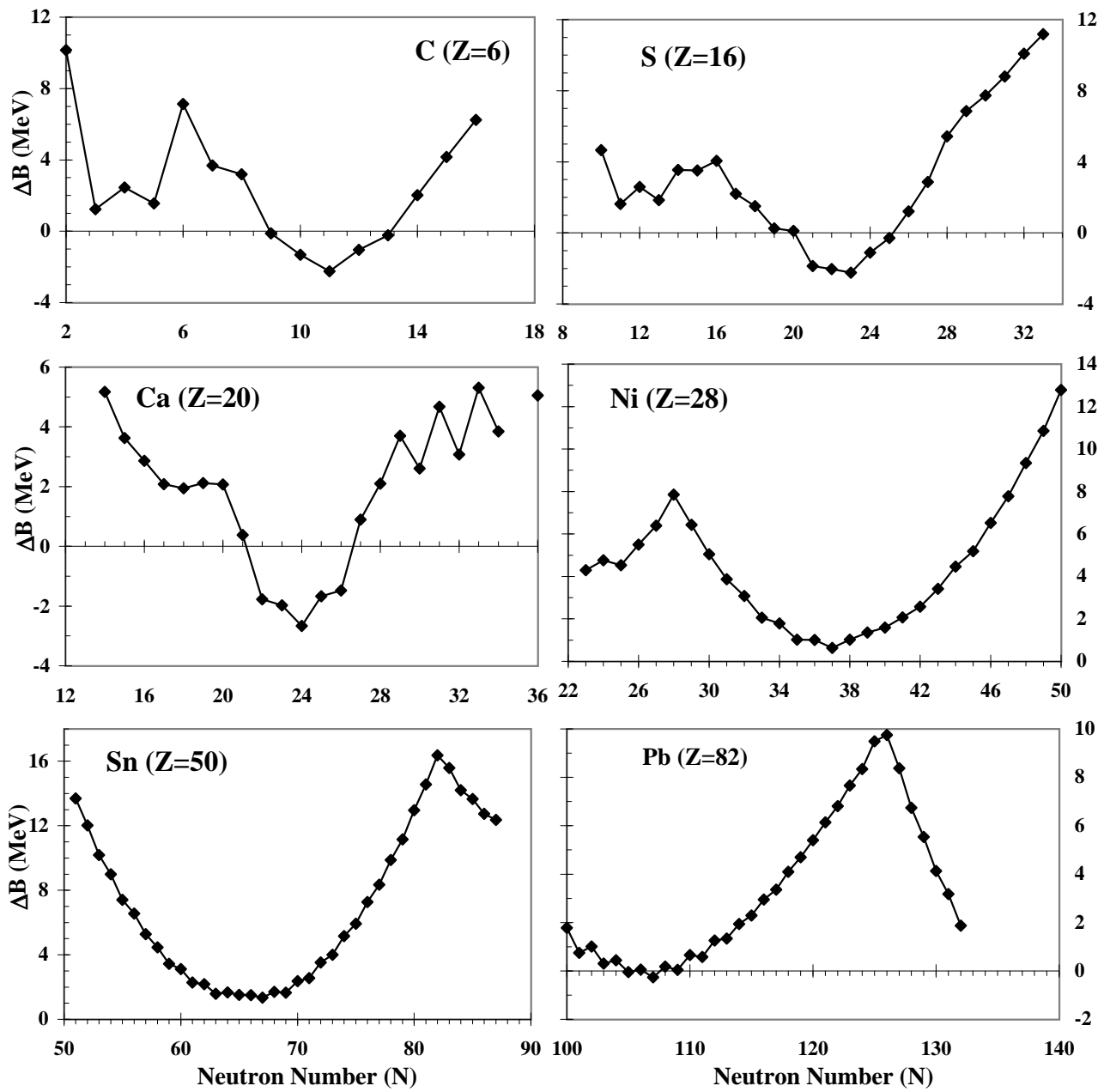


Fig. 6

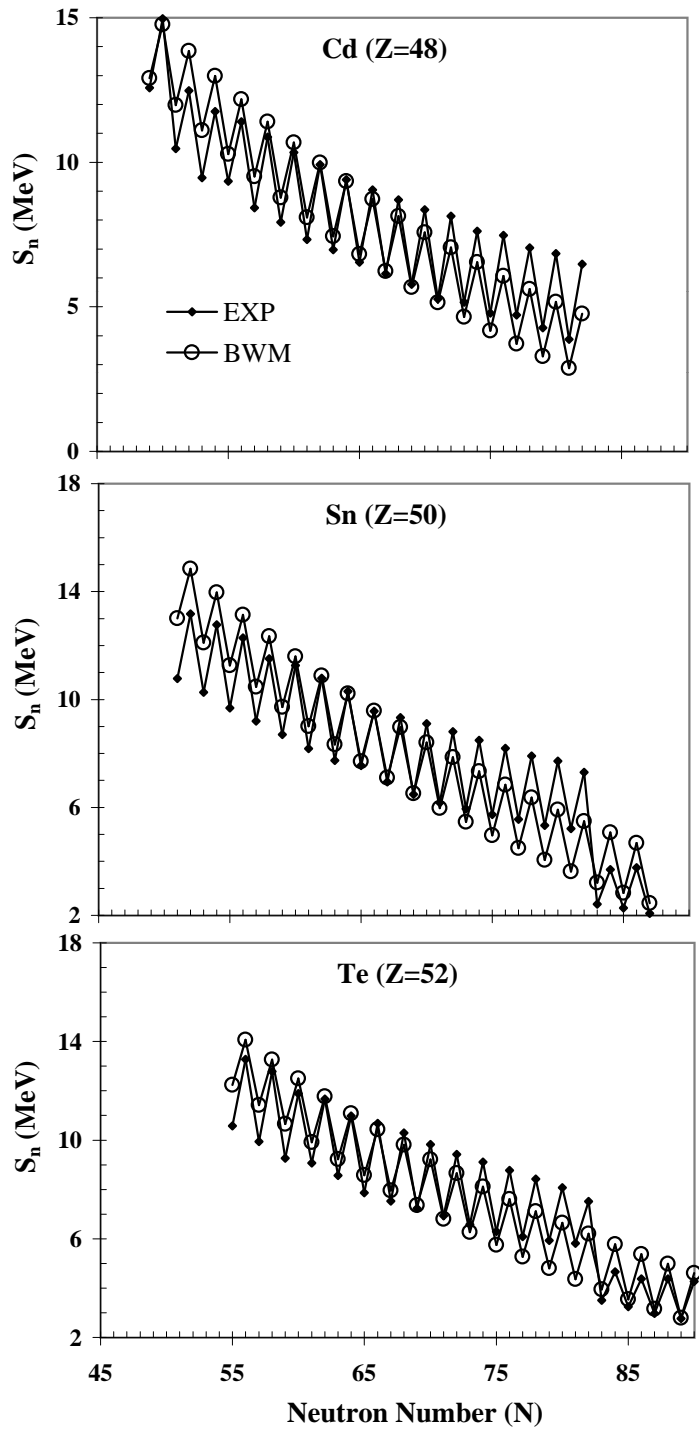


Fig.7